

7-15-1989

Double Hole Cyclotron-Resonance in Zero-Gap HgTe-CdTe Superlattices

J. R. Meyer

Robert Wagner

Worcester Polytechnic Institute, rwagner@wpi.edu

F. J. Bartoli

C. A. Hoffman

L. Ramdas Ram-Mohan

Worcester Polytechnic Institute, lrram@wpi.edu

Follow this and additional works at: <http://digitalcommons.wpi.edu/chemicalengineering-pubs>



Part of the [Chemical Engineering Commons](#)

Suggested Citation

Meyer, J. R., Wagner, Robert, Bartoli, F. J., Hoffman, C. A., Ram-Mohan, L. R. (1989). Double Hole Cyclotron-Resonance in Zero-Gap HgTe-CdTe Superlattices. *Physical Review B*, 40(2), 1388-1391.

Retrieved from: <http://digitalcommons.wpi.edu/chemicalengineering-pubs/15>

This Article is brought to you for free and open access by the Department of Chemical Engineering at DigitalCommons@WPI. It has been accepted for inclusion in Chemical Engineering Faculty Publications by an authorized administrator of DigitalCommons@WPI.

Double hole cyclotron resonance in zero-gap HgTe-CdTe superlattices

J. R. Meyer, R. J. Wagner, F. J. Bartoli, and C. A. Hoffman
Naval Research Laboratory, Washington, D.C. 20375

L. R. Ram-Mohan
Worcester Polytechnic Institute, Worcester, Massachusetts 01609
 (Received 9 March 1989)

Magnetic-field-dependent band structures for HgTe-CdTe superlattices with zero band gap have been calculated by the transfer-matrix method. We find that there is an unusual mixing of cyclotron resonance and interband transitions. The analysis predicts that the hole cyclotron resonance should display two peaks corresponding to transitions in different regions of the Brillouin zone. Agreement with recent data showing a double peak in the Faraday geometry is quite good.

Previous investigations have demonstrated that the HgTe-CdTe superlattice band structure displays a number of interesting properties in the regime of zero energy gap.¹ For example, alignment of the conduction and valence bands is indirect, the effective masses of both electrons and holes are significantly broadened (i.e., carriers with a wide range of masses coexist in the superlattice), and the hole dispersion is extremely nonparabolic. It has recently been observed that these features are manifested in the experimental free-carrier transport data.² In the present work, we show that further effects are expected when a magnetic field is introduced. Although calculations of field-dependent band structures for HgTe-CdTe superlattices have previously appeared in the literature,³⁻⁵ there has been no discussion of the special properties which arise when the band gap is at or near zero. These properties are of particular interest because recent far-infrared magneto-optical measurements on *p*-type HgTe-CdTe superlattices^{6,7} with zero energy gap have produced features which cannot be explained by previous theories. In particular, the magnetoabsorption spectra for Faraday geometry display two peaks, both of which are allowed in the hole cyclotron resonance sense of circular polarization.

HgTe-CdTe superlattice band structures have been calculated using a transfer-matrix algorithm which has been described in detail elsewhere.⁸ Within the envelope function approach, an 8-band $\mathbf{k}\cdot\mathbf{p}$ model is employed rather than the 6-band approximations used by previous investigators.^{3,4} For zero magnetic field, the results agree well with band structures obtained by the tight-binding method.^{1,9} In the calculations discussed below, strain is included, a valence-band offset of 350 meV is employed, and it is assumed that the barriers contain 15% HgTe.¹⁰

Before discussing the *B*-dependent band structure, we briefly review the case of HgTe-CdTe superlattices in the absence of a magnetic field.^{2,11} If the well thickness d_W is relatively narrow, the superlattice will have a positive energy gap E_g , i.e., for any growth-direction wave vector k_z , the conduction band *E*1 will be at a higher energy than the heavy-hole band HH1 (for large valence-band offsets the light-hole-like band LH1 is well below the band edge).¹¹ As d_W is increased, E_g decreases until finally *E*1

and HH1 meet and then cross in the k_z direction at some value k_{zc} . For $k_z < k_{zc}$, HH1 becomes the conduction band and *E*1 the valence band. Although $E_g \approx 0$, the alignment is indirect since the conduction-band minimum is at $k_z < k_{zc}$, while the valence-band maximum is at $k_z < k_{zc}$. Electrons and holes with a wide range of masses coexist (mass broadening) because HH1 is nearly degenerate in k_z and the in-plane effective mass at a given k_z is proportional to the energy separation between *E*1 and HH1, which varies significantly with k_z . Although $E_g \approx 0$ over the range of well widths for which *E*1 and HH1 cross, at sufficiently large d_W the entire *E*1 band lies below HH1 and there is again an energy gap^{2,12} (at $k_x = 0$, but not necessarily for all in-plane wave vectors).

Previous studies of HgTe-CdTe superlattices in the presence of a magnetic field along the growth direction³⁻⁵ have shown that when $E_g > 0$, the arrangement of the Landau levels is qualitatively similar to that obtained for wider-gap III-V heterostructures, such as GaAs-Ga_{1-x}Al_xAs.⁸ Both *E*1 and HH1 are composed of two concurrent series of levels, labeled primed and unprimed, which correspond to the two 4-band sets of states discussed for bulk semiconductors by Pidgeon and Brown.¹³ In lowest order, magneto-optical transitions between the primed and unprimed series are forbidden. The selection rule for σ^\pm polarization is $\Delta n = \pm 1$ for either interband or intraband (cyclotron resonance) transitions, although the two are easily distinguishable because the energy scales are much different and because interband processes go between *E*1 and HH1 while cyclotron resonance occurs within either *E*1 or HH1. We will see below that in the zero-gap regime, the distinction between interband and intraband processes becomes much less clear.

Figure 1 shows energy bands calculated for $d_W = 78 \text{ \AA}$ ($N_W = 24$ monolayers), $d_B = 45 \text{ \AA}$ ($N_B = 14$), and $B = 1 \text{ kG}$. Note that the independent variable is a growth-direction wave vector, since many of the most interesting properties of the zero-gap regime originate from the strong dependence of the bands on k_z . The bands labeled 0 and -2' represent ground-state Landau levels for *E*1 and HH1, respectively, and their dependences on k_z are quite similar to those in the absence of a magnetic field. The crossing at $k_{zc} \approx 0.13\pi/d$ separates the region in which

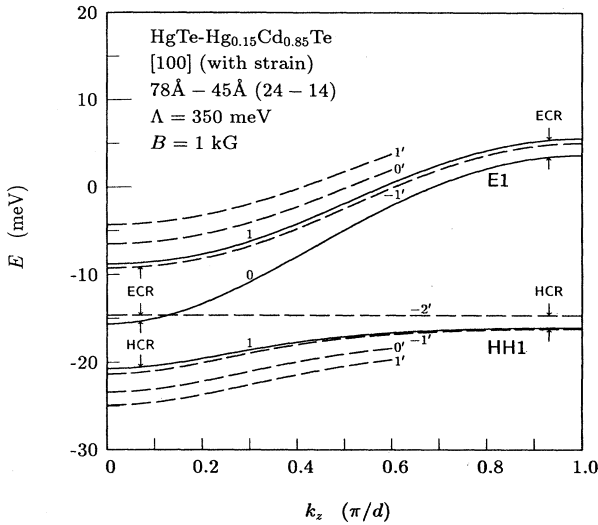


FIG. 1. Superlattice Landau levels vs growth-direction wave vector at $B=1$ kG and $T=0$. The unprimed (solid curves) series 2, 3, ... continues above and below the levels shown in a manner similar to the primed (dashed curves) series. In lowest order, only transitions within the dashed or solid series are allowed.

$-2'$ is a conduction band and 0 is a valence band from that in which their roles are reversed. However, $-2'$ and 0 are the only two bands which cross,¹⁴ since the other levels remain either above or below the two ground states. It is as if a given higher-order band is an excited state of one ground state at small k_z , but the other at large k_z . This arrangement also leads to a mixing of the conventional distinctions between interband and cyclotron resonance processes. For example, consider transitions between 0 and the lower of the two bands labeled 1. Since 0 is a valence band at small k_z , this process has the character of hole cyclotron resonance in that region (see the arrows in Fig. 1). However, 0 is a conduction band at large k_z and there the same transition clearly resembles interband absorption. Similarly, transitions between $-2'$ and the upper of the two bands labeled $-1'$ resemble electron cyclotron resonance at small k_z , but interband absorption at large k_z . On the other hand, all higher-order processes maintain a constant character, e.g., the transition $-1'$ (upper) \rightarrow $0'$ (upper) is always electron cyclotron resonance. Note that due to nonparabolicity, the resonance energy $\hbar\omega_c$ is a factor of 2 larger for $-2' \rightarrow -1'$ than it is for $-1' \rightarrow 0'$ (at small k_z).

Thus, one has the potential for a large variety of magneto-optical transitions. Which ones are observable in a given superlattice at a given magnetic field will depend in part on the location of the Fermi level. In order to compare with recent hole cyclotron resonance data, we will emphasize transitions which would be expected in a p -type sample. However, the analysis for n -type superlattices would be similar, since any hole transition shown in Fig. 1 has an electron counterpart (the two are not strictly analogous because of the much larger curvature of the $E1$ band with k_z). Let us assume for simplicity that the tem-

perature is zero and that the Fermi level is at -16 meV, i.e., just below the 0 level at $k_z=0$ and between the $-2'$ and $-1'$ (lower) levels at $k_z=\pi/d$. There will be a large number of possible interband transitions of the type $-1'$ (lower) \rightarrow $0'$ (upper), $0'$ (lower) \rightarrow $-1'$ (upper), etc., which satisfy the $\Delta n = \pm 1$ selection rule. However, there are only two allowed processes coupling a full initial state and an empty final state which have energy differences in the range accessed by the far-infrared magneto-optical experiments of interest,^{6,7} i.e., less than ≈ 14 meV: 1 (lower) \rightarrow 0 and $-1'$ (lower) \rightarrow $-2'$. Note that both of these transitions have ΔE which vary considerably with k_z , i.e., neither will be associated with a single, sharply defined resonance. Instead, there will be a continuous spectrum of transition energies which correspond directly to the mass-broadening effect discussed previously in connection with zero-field band structures.² Assuming that scattering does not cause too much additional broadening (i.e., $\omega_c\tau > 1$), the maxima of the spectrum will occur near those extremal regions for which ΔE changes most slowly with k_z . (The situation is somewhat similar for interband transitions in InAs-GaSb superlattices.¹⁵) An examination of Fig. 1 shows that there are primarily two such regions in the present example, namely those which have been labeled HCR. Although there is also a third possibility: interbandlike transitions of the type $-1'$ (lower) \rightarrow $-2'$ at small k_z , Fig. 1 shows that the curvature of $\Delta E(k_z)$ is greater in that case. We will find below that this process does not necessarily lead to a separate absorption peak.

In order to demonstrate explicitly that multiple maxima should occur, we now perform a simple magnetotransmission spectrum calculation for input parameters appropriate for the example discussed in the previous paragraph. Use of the Drude form for the frequency-dependent conductivity reveals that the power absorbed is approximately¹⁶

$$P(\omega) = \frac{1}{2} |\epsilon|^2 \frac{\sigma_0}{1 + (\omega\tau - \omega_c\tau)^2}, \quad (1)$$

where ϵ is the optical electric field, $\sigma_0 = pe^2\tau/m_x$ is the zero-frequency conductivity, τ is the momentum relaxation time, $m_x = eB/\omega_c$ is the in-plane effective mass, and ω is the optical frequency. The cyclotron frequency may be obtained directly from Fig. 1 by equating $\hbar\omega_c$ to ΔE , the energy difference between Landau levels involved in a given transition. The hole density is

$$p = \frac{eB}{2\pi^2\hbar} \sum_n \int_0^{\pi/d} dk_z f_0, \quad (2)$$

where f_0 is the Fermi distribution function and the summation is over hole Landau levels. Substituting for σ_0 in Eq. (1), we obtain

$$P(\omega) \sim \int_0^{\pi/d} \frac{\omega_c \tau dk_z}{1 + (\omega\tau - \omega_c\tau)^2}, \quad (3)$$

where for simplicity we assume that only the highest-hole Landau level is occupied. Numerical evaluation of this expression leads to the transmission spectrum shown in Fig. 2. A relaxation time of 1 ps was employed,¹⁷ which is

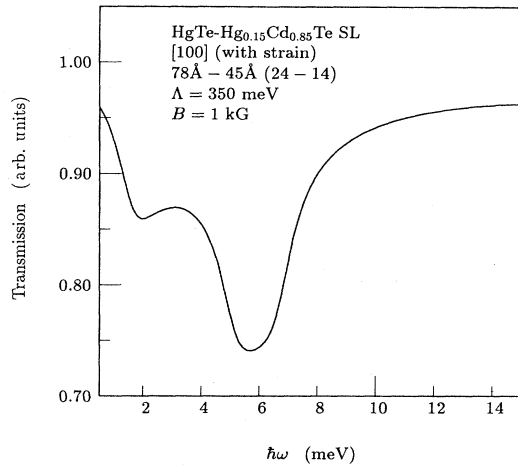


FIG. 2. Calculated magnetoabsorption for lowest-level Landau transitions, ignoring statistical factors and assuming $\tau = 1$ ps.

just slightly greater than the value 0.3 ps estimated experimentally by Perez *et al.*⁶ We see that there are in fact two absorption peaks, corresponding to the two HCR transitions indicated in Fig. 1. The peak energies of 2.0 and 5.8 meV are slightly larger than the extremal (zone boundary) values for ΔE : 1.5 and 5.1 meV. Since ΔE for both transitions increase as one moves away from the zone boundaries, it should not be surprising that the “averaged” values are higher than the extremal values. On the other hand, the interband process $-1'$ (lower) $\rightarrow 2'$ (small k_z), which was discussed in the previous paragraph, is not resolvable as a separate peak. Instead, it is part of the high-energy tail of the 5.8-meV peak.

Although our analysis is somewhat simplified since we have not incorporated overlap integrals or accounted in detail for the initial and final-state occupation statistical factors, we can nonetheless perform a first-order estimate of the magnetoabsorption peak energies. These will then be compared with the recent experimental results of Perez *et al.*,⁶ who studied a *p*-type HgTe-CdTe superlattice with nominal well and barrier widths of 23 and 14 monolayers (± 2 monolayers). Because the band-structure calculation predicts a small positive energy gap (3 meV) for these parameters, we have increased the well width by 1 monolayer to make the superlattice semimetallic.¹⁸

As in the theoretical spectrum shown in Fig. 2, the Faraday-geometry data yielded two absorption peaks, which are both allowed for circular polarization in the hole cyclotron resonance sense (in the experiment, $\hbar\omega$ is held fixed and one finds the peak in magnetic field). In Fig. 3, the experimental results for transition energies versus magnetic field are compared with calculated values based on the zone-boundary energy differences. The theoretical curves are seen to quite accurately reproduce the main features of the data, including the nonparabolicity. It should be remembered that the only adjusted parameter in the calculation was an increase in the well width by 1 monolayer. Furthermore, we saw above that

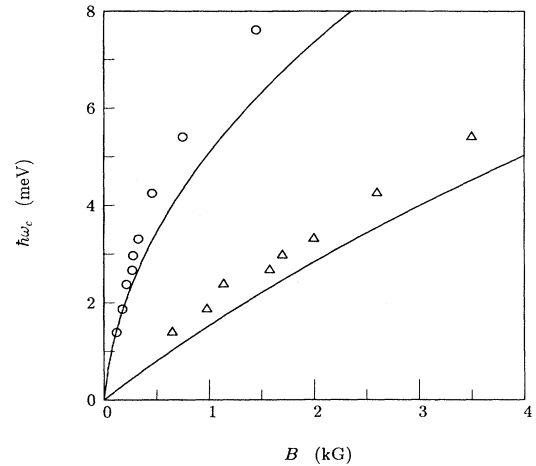


FIG. 3. Experimental (Ref. 6) (points) and theoretical (curves) hole cyclotron resonance energies vs magnetic field. The theoretical values are based on lowest-order Landau-level transitions at the zone boundaries for a HgTe-Hg_{0.15}Cd_{0.85}Te superlattice with $N_W = 24$ and $N_B = 14$.

the extremal resonance energies underestimate the expected peak values, so a more detailed calculation may improve the agreement between theory and experiment.

While Perez *et al.* had identified the higher-energy transition as hole cyclotron resonance, the lower-energy line was previously unexplained. Spin resonance was suggested because the variation with magnetic-field angle appeared to link this line to a Voigt-geometry resonance with $\epsilon \parallel \mathbf{B}$ selection (whereas the higher-energy line was linked to a Voigt resonance with $\epsilon \perp \mathbf{B}$ selection, as generally holds for cyclotron resonance in bulk semiconductors). In a small-gap semiconductor, one expects the spin splitting to be comparable to the Landau splitting.¹⁹ For the band structure shown in Fig. 1, the lowest-order spin resonance transition is $-1'$ (lower at small k_z , upper at large k_z) $\rightarrow 0$. Since the two $-1'$ bands are in close proximity to the 1 bands, the ΔE for spin resonance is quite similar to the hole cyclotron resonance energy at small k_z and the electron cyclotron resonance energy at large k_z . Therefore, if the sample is *p* type one expects the spin resonance (which may be weak since the process is forbidden in lowest order) to be much closer to the higher energy rather than the lower energy of the two experimentally observed peaks. Although the present theory appears to account for both of the lines seen in Faraday geometry (both are interpreted as hole cyclotron resonance), the reason for the observed Voigt-geometry selection rules remains unclear. The present band-structure calculations have not yet been generalized to account for arbitrary magnetic-field direction.

Summarizing, we have presented the first theoretical study of the influence of a magnetic field on the band structure of HgTe-CdTe superlattices with zero energy gap. As in the absence of a magnetic field, the dependence on growth-direction wave vector is found to be crucial. While the ground-state Landau levels are similar to the bands at $B=0$, the excited levels change from $E1$ to

HH1 character (or vice versa) as k_z is varied. This leads to a mixing of interband and intraband (cyclotron resonance) transitions. The variety of possible magneto-optical transitions is quite large, and the transition energies span a continuous range. However, it is explicitly demonstrated that magnetoabsorption peaks should occur near the energy differences for extremal transitions at the zone boundaries, where ΔE does not change rapidly with k_z . For p -type samples it is predicted that there should be double cyclotron resonance peaks, one associated with transitions near $k_z = 0$ and the other with transitions near

$k_z = \pi/d$. The dependences of both peak energies on magnetic field are found to be in good agreement with the experimental results of Perez *et al.* We are thus able to account for the previously unexplained lower-energy peak.

We thank K. H. Yoo and J. K. Furdyna for valuable discussions. This research was supported by the Strategic Defense Initiative Office of Innovative Science and Technology and managed by the Naval Research Laboratory.

-
- ¹J. R. Meyer, C. A. Hoffman, F. J. Bartoli, J. W. Han, J. W. Cook, Jr., J. F. Schetzina, X. Chu, J. P. Faurie, and J. N. Schulman, *Phys. Rev. B* **38**, 2204 (1988).
- ²C. A. Hoffman, J. R. Meyer, F. J. Bartoli, J. W. Han, J. W. Cook, Jr., J. F. Schetzina, and J. N. Schulman, *Phys. Rev. B* **39**, 5208 (1989).
- ³J. M. Berroir, Y. Guldner, J. P. Vieren, M. Voos, and J. P. Faurie, *Phys. Rev. B* **34**, 891 (1986).
- ⁴Z. Yang, M. Dobrowolska, H. Luo, J. K. Furdyna, and J. T. Cheung, *Phys. Rev. B* **38**, 3409 (1988).
- ⁵K. H. Yoo, R. L. Aggarwal, and L. R. Ram-Mohan, *J. Vac. Sci. Technol.* **A7**, 415 (1989).
- ⁶J. M. Perez, R. J. Wagner, J. R. Meyer, J. W. Han, J. W. Cook, Jr., and J. F. Schetzina, *Phys. Rev. Lett.* **61**, 2261 (1988).
- ⁷M. Dobrowolska, T. Wojtowicz, J. K. Furdyna, O. K. Wu, J. N. Schulman, J. R. Meyer, C. A. Hoffman, and F. J. Bartoli (unpublished).
- ⁸L. R. Ram-Mohan, K. H. Yoo, and R. L. Aggarwal, *Phys. Rev. B* **38**, 6151 (1988).
- ⁹J. N. Schulman and Y.-C. Chang, *Phys. Rev. B* **33**, 2594 (1986).
- ¹⁰Justification for these input assumptions is discussed in detail in Ref. 2.
- ¹¹J. R. Meyer, C. A. Hoffman, F. J. Bartoli, and J. N. Schulman, *Phys. Rev. B* **38**, 12457 (1988).
- ¹²N. F. Johnson, P. M. Hui, and H. Ehrenreich, *Phys. Rev. Lett.* **61**, 1993 (1988).
- ¹³C. R. Pidgeon and R. N. Brown, *Phys. Rev.* **146**, 575 (1966).
- ¹⁴This rule may be affected by the generality of the set of basis functions employed.
- ¹⁵J. C. Maan, Y. Guldner, J. P. Vieren, P. Voisin, M. Voos, L. L. Chang, and L. Esaki, *Solid State Commun.* **39**, 683 (1981).
- ¹⁶K. Seeger, *Semiconductor Physics* (Springer-Verlag, New York, 1973), p. 394.
- ¹⁷If $\tau \approx 0.3$ ps is employed, the 5.8-meV peak in Fig. 2 is still sharp, but the 2.0-meV feature ceases to have a resolvable peak. The experimental estimate for τ may have been low since it was based on the assumption that the entire linewidth is due to scattering rather than mass broadening.
- ¹⁸The corresponding theoretical curves for $N_W = 23$ rather than 24 are quite similar to those shown in Fig. 3, except that both resonance energies are lower by 10–30%. If N_W is increased above 24, the higher-energy resonance moves down somewhat while the lower-energy resonance moves up in energy. Beyond this, the statistical occupation factors can be affected considerably as N_W is varied.
- ¹⁹For example, see Eqs. (21) and (22) of M. H. Weiler, in *Semiconductors and Semimetals*, edited by R. K. Willardson and A. C. Beer (Academic, New York, 1981), p. 119.